YEAR 2 PROGRESS REPORT FOR NASA GRANT NNX08AM56G

SCOTT DENNING

MODELING THE GLOBAL ATMOSPHERIC CARBON CYCLE IN PREPARATION FOR OCO DATA

1. Global Simulations of Atmospheric CO2 using GEOS-5 Products

We have updated the SiB-PCTM simulation experiments to the latest version of GEOS-DAS, version 5.1.0 of the GEOS general circulation model (GEOS5). GEOS5 is a new global reanalysis product from Goddard that resolves atmospheric processes at the mesoscale, using horizontal resolution of 0.5 latitude x 0.67 longitude (including 72 vertical levels), making possible global mesoscale simulations of atmospheric carbon. In the poster, we tested sensitivity of carbon flux calculations in SiB and synoptic variations of atmospheric CO2 in PCTM to GEOS4 (1.0 latitude x 1.25 longitude x 25 vertical levels) and GEOS5, to demonstrate: 1) the influence of spatial resolution on atmospheric CO2 and, 2) the influence of surface meteorology on GPP.

On the land surface side, with regard to GPP, owing to the strong sensitivity of SiB GPP to environmental factors such as atmospheric moisture, precipitation, and temperature, we find global, regional, and annual changes in GPP between reanalysis products. Enhanced moisture (in the atmosphere and soil) and decreased surface temperature in GEOS5 in Northern Hemisphere upper latitudes promotes more favorable environments for photosynthesis. Overall, global GPP increases from 111 GtC/yr using GEOS4 to 122 GtC/yr in GEOS5, which is consistent with estimates from the MODIS algorithm (Zhao et al., 2005).

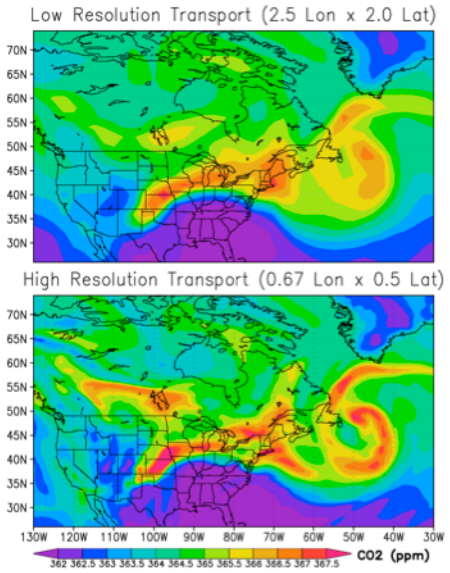

Figure 0: Simulated X_{CO2} for March 5, 2004 using two different grids

On the atmospheric side, we performed experiments to determine whether day-to-day variations in atmospheric CO2 are more sensitive to land surface flux (based on SiB GPP calculated using GEOS4 and GEOS5, assuming constant transport) or changes in transport resolution (based on transport by GEOS4 and GEOS5, assuming constant GPP). Using time lag correlations of model output to surface observations over North America, Europe, and several remote sites, we find in general stronger correlations at zero time lag when moving the transport driver from GEOS4 to GEOS5. Changes in SiB GPP seem to have negligible impact on these correlations.

Figure 1 compares snapshots of column-integrated CO2 mixing ratio as simulated by SiB-PCTM using the 2x2.5 GEOS4 and the 0.5x0.67 GEOS5

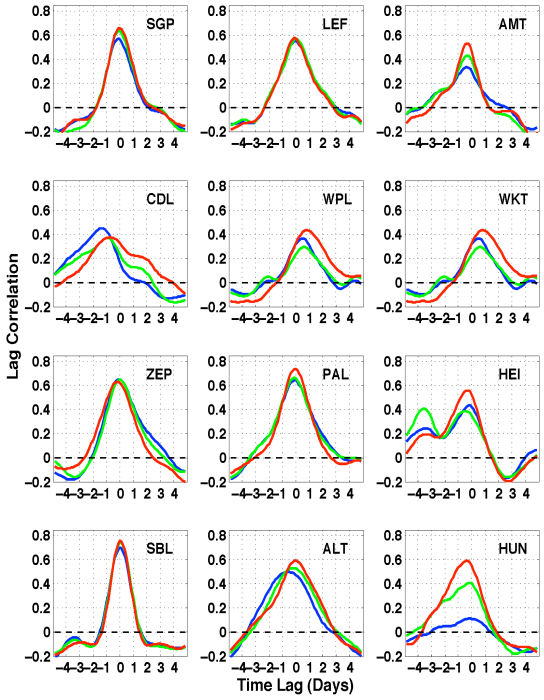

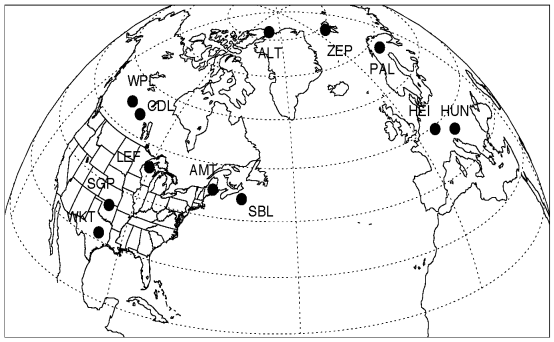

Figure 2: Lagged correlation analysis of synoptic variations of simulated and observed CO_2 at 12 in-situ stations (locations shown above). Abscissa is time lag (days). Blue is driven by GEOS-4 at 2°x2.5°, green uses GEOS4 at 1°x1°, and red uses GEOS-5 at 0.5°x0.67°

transport. Much tighter gradients and spatial detail appear in the finer-scale simulation. To evaluate the realism of these simulations, we compared the timeseries of simulated surface CO2 with in-situ observations for 12 stations in the Northern Hemisphere (Fig 2). Autocorrelation with the observations is higher at almost all sites using the finer-resolution meteorology, and lags are improved at some sites.

To interpret the sensitivity of day-to-day variations in atmospheric CO2 to transport, we use Eddy Decomposition of atmospheric transport to break down the meridional circulation into large scale transport by the mean meridional circulation (e.g., Hadley Cell), regional transport by stationary eddies (e.g., Bermuda High, Icelandic Low, etc), and regional transport by transient eddies (storm tracks). We believe it is transport along storm tracks that have the most influence on high frequency midlatitude variations. Using this analysis framework, we find sensitivity of transport by Transient Eddies to transport resolution. (Fig 3).

Using this method, we investigated the differences in transport mechanisms between the coarse (2x2.5) and fine (0.5x0.67) models (Fig 4). As expected, total meridional transport is not substantially different among the models, but there is a tradeoff among the strengths of different mechanisms. In the fine-scale transport model, meridional transport by the transient eddies (baroclinic waves) is stronger due to better resolution of both tracer gradients amd frontal meteorology. This is compensated by stronger symmetric transport in the Mean Meridional Ferrel Cell. There are important implications for interpretation of satellite CO2 products because of cloud masking in frontal zones (Fig 5) where the satellite will never sample.

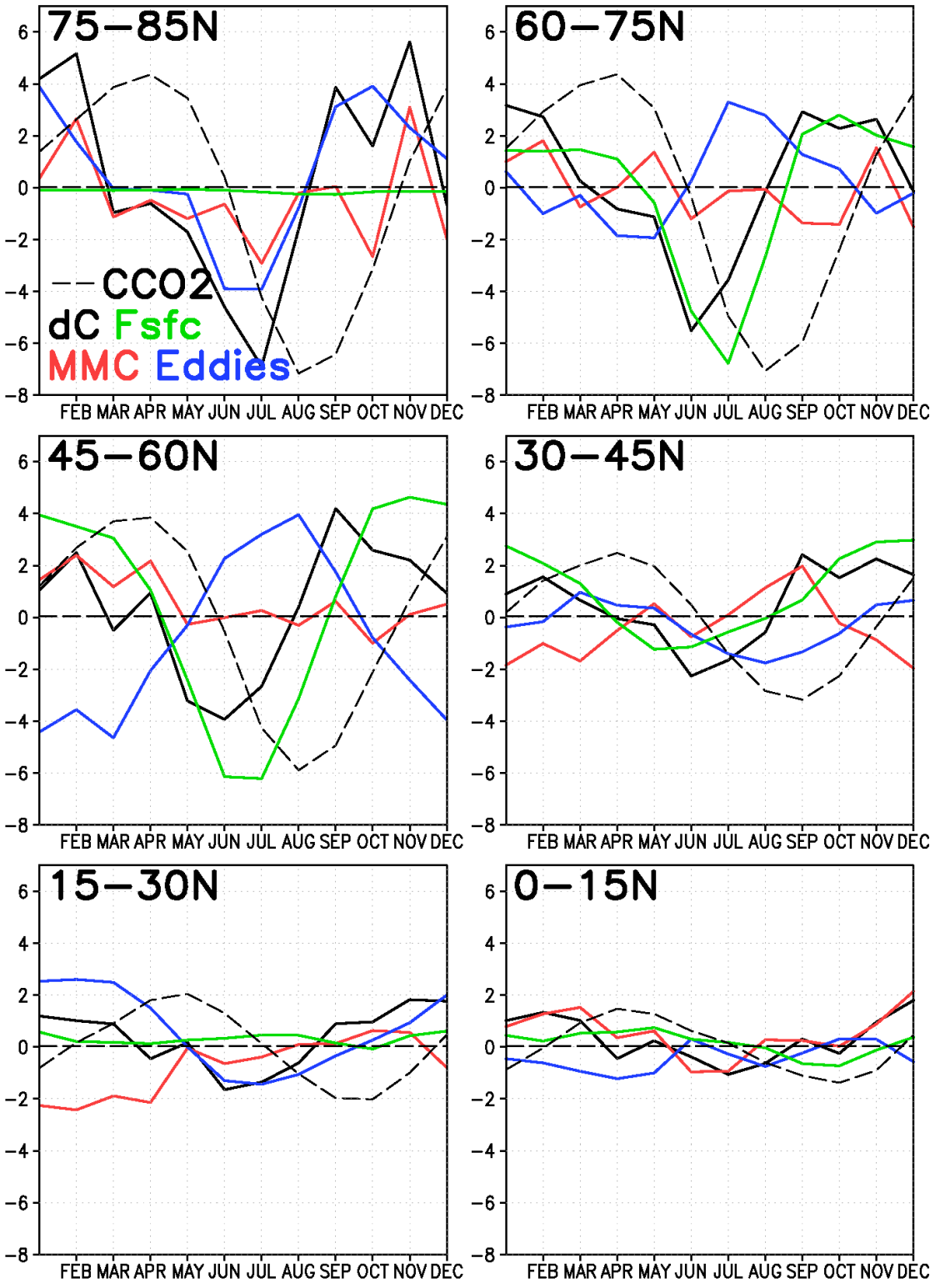

Figure 3: Vertically-integrated CO2 budgets (ppm/month) over zonal bands of the atmosphere.

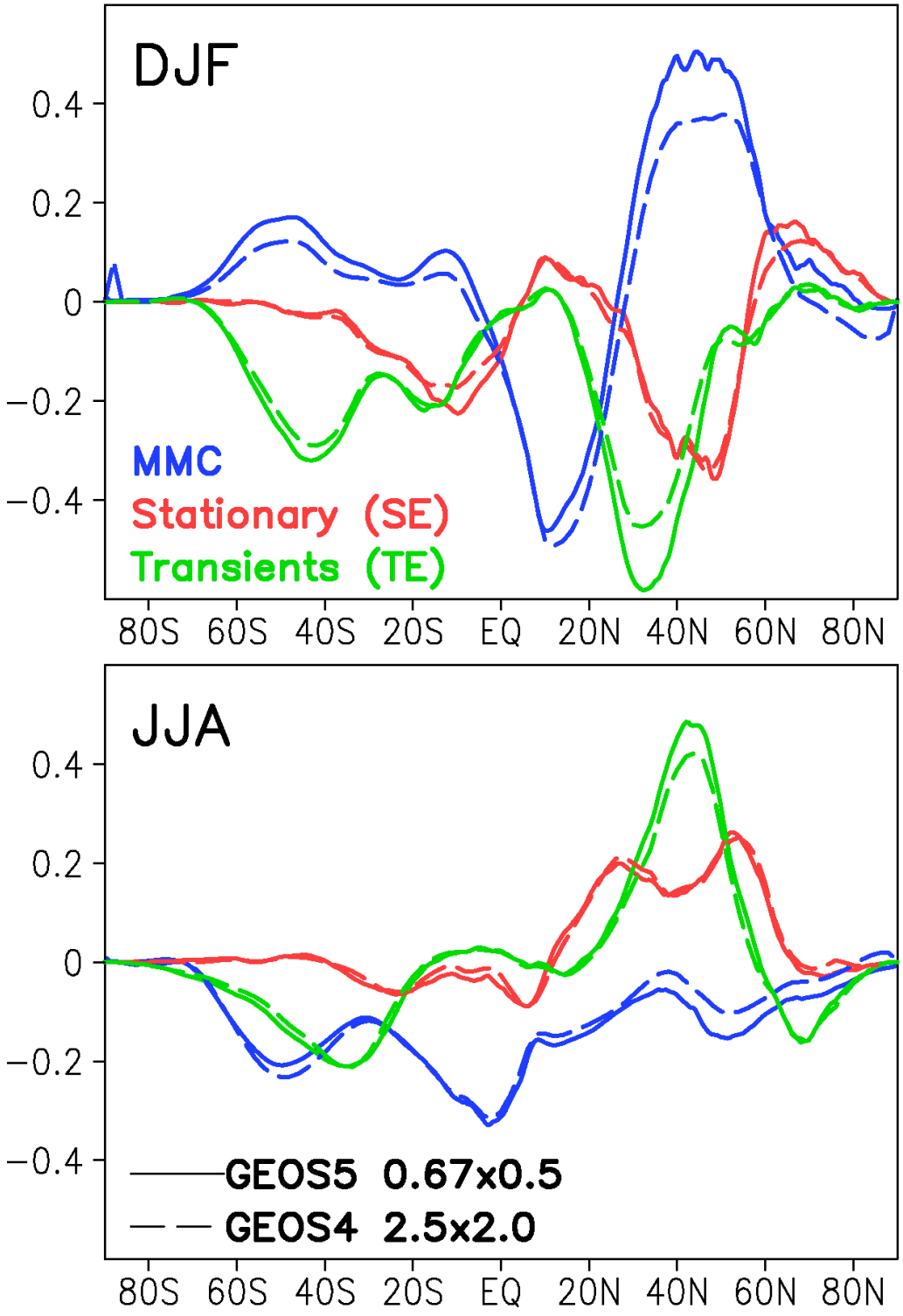

Figure 4: Meridional transport (PgC/month) by the mean meridional circulation (blue), stationary eddies (red), and transients (green) as simulated in SiB-PCTM using 2x2.5 degree (dashed) and 0.5x0.67 degree (solid) meteorology.

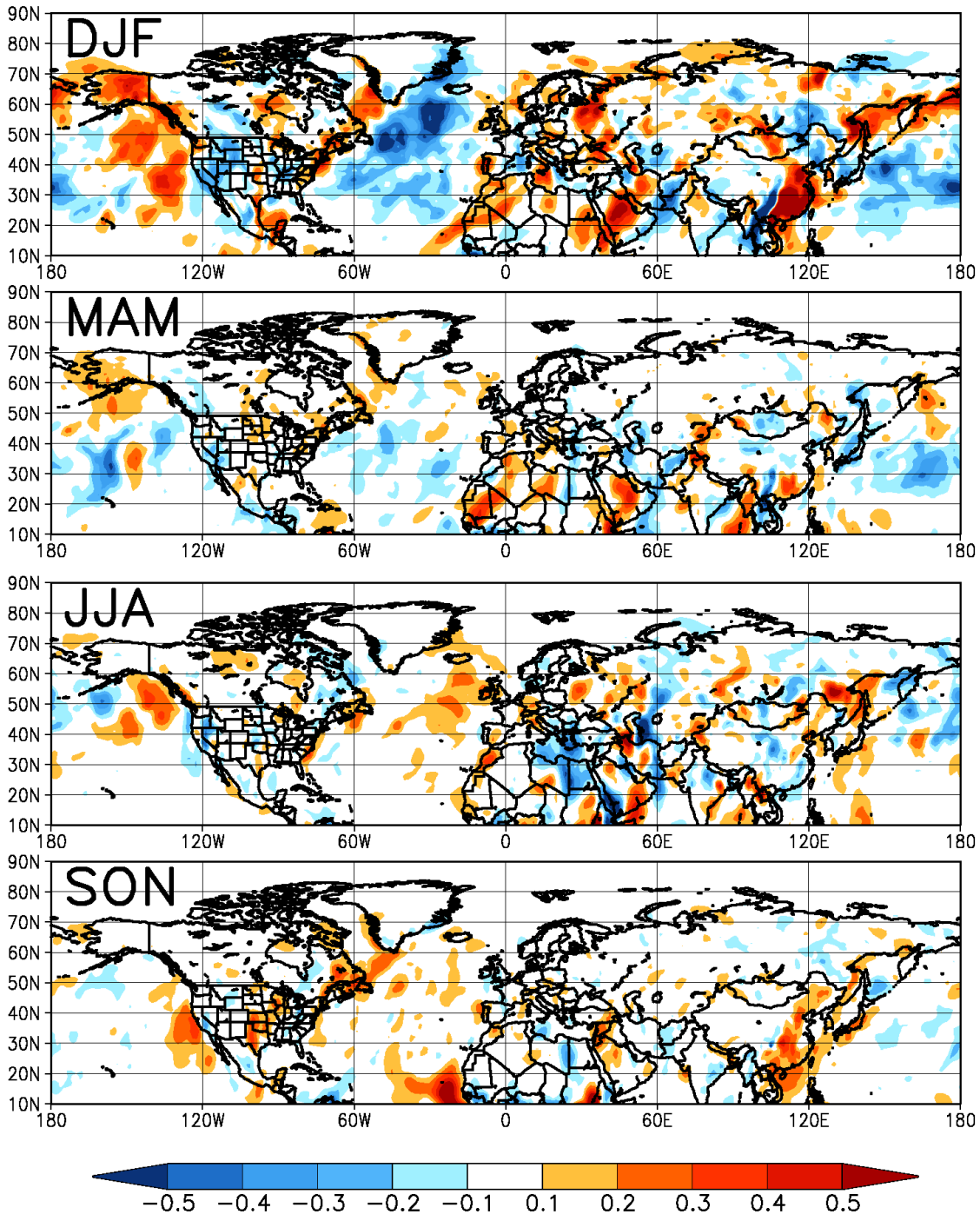

Figure 5: Difference in meridional transport (PgC/month) by stationary and transient eddies as simulated by SiB-PCTM using 2x2.5 degree vs 0.5x0.67 degree meteorology.

2. Global Carbon Flux Estimation from In-Situ CO2 Data Using Ensemble Data Assimilation with SiB-PCTM and the MLEF

We used our data assimilation system (MLEF) to estimate global carbon fluxes using the existing in-situ observation network. We compared our results with the CarbonTracker, another data assimilation system. According to uncertainty reduction map shown in Figure 6, densely observed North American and European

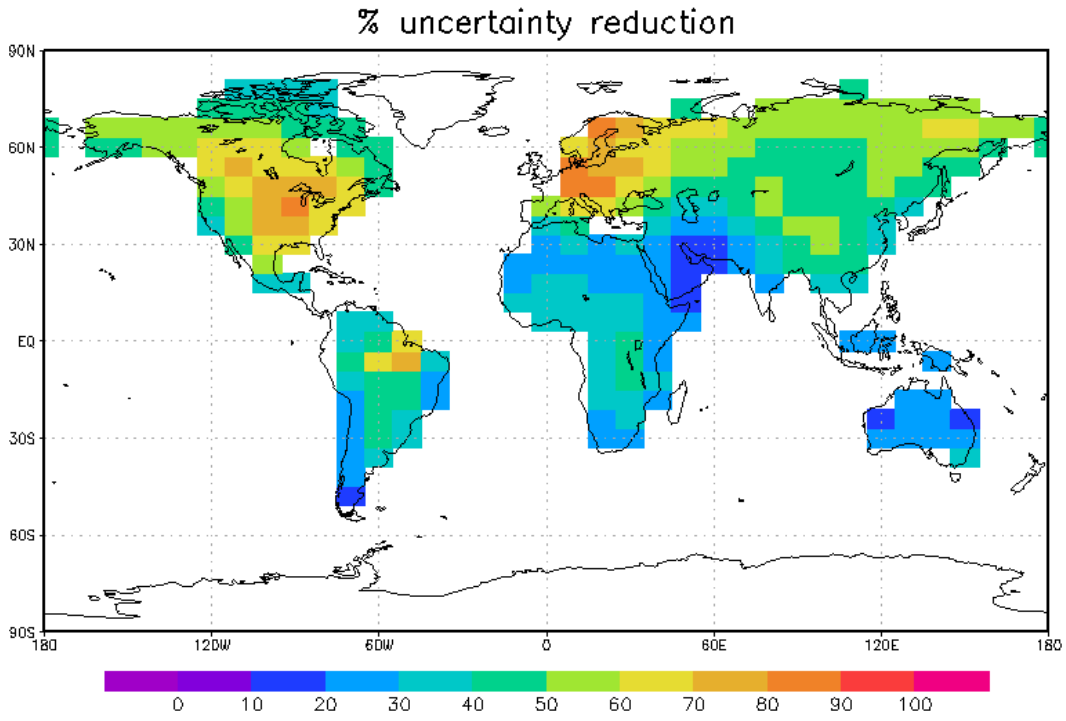

Figure 6: Annual mean uncertainty reduction in terrestrial NEE from assimilation of in-situ CO2 data.

regions show good constrain on flux estimates. Hence we chose to show results only from those regions. Estimated fluxes for years 2003 and 2004 were similar when aggregated up into large TransCom regions (Figure 7). However the spatial patterns were quite different in these regions (Figure 8). These differences could be due to the differences in the models. CarbonTracker uses 3-hourly fluxes as prior whereas MLEF uses SiB3 hourly fluxes. Also, the CarbonTracker solves for large ecoregions as their basis functions, but we solve the problem in grid scale (10 longitude $\times$ 6 latitude).

(a)

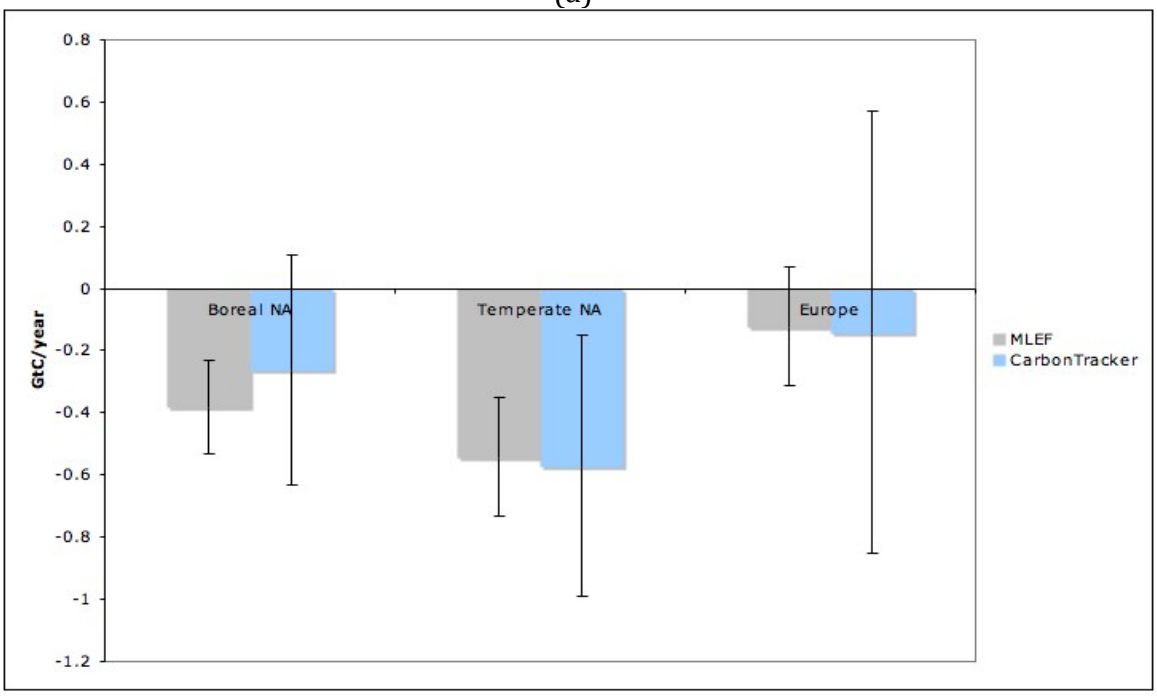

(b)

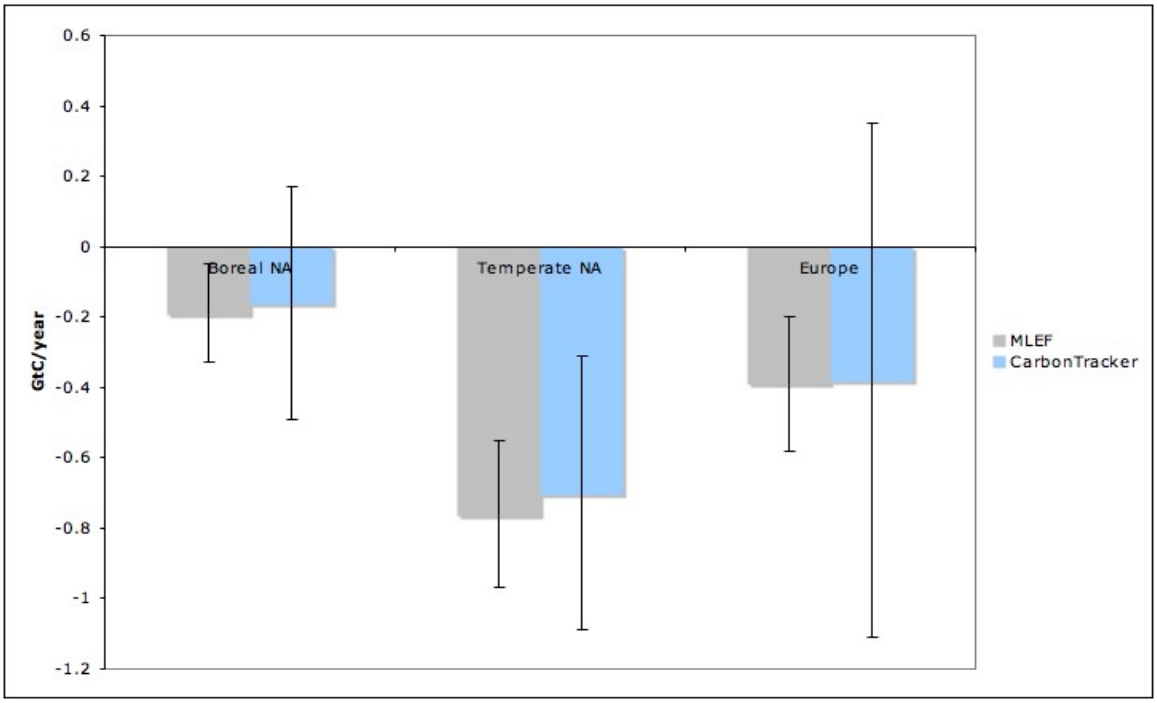

Figure 7. Mean annual NEE with 1-σ error bars aggregated to TransCom regions; Boreal North America, Temperate North America, and Europe, estimated by MLEF and CarbonTracker (a) for 2003 and (b) for 2004. Units: GtC/year.

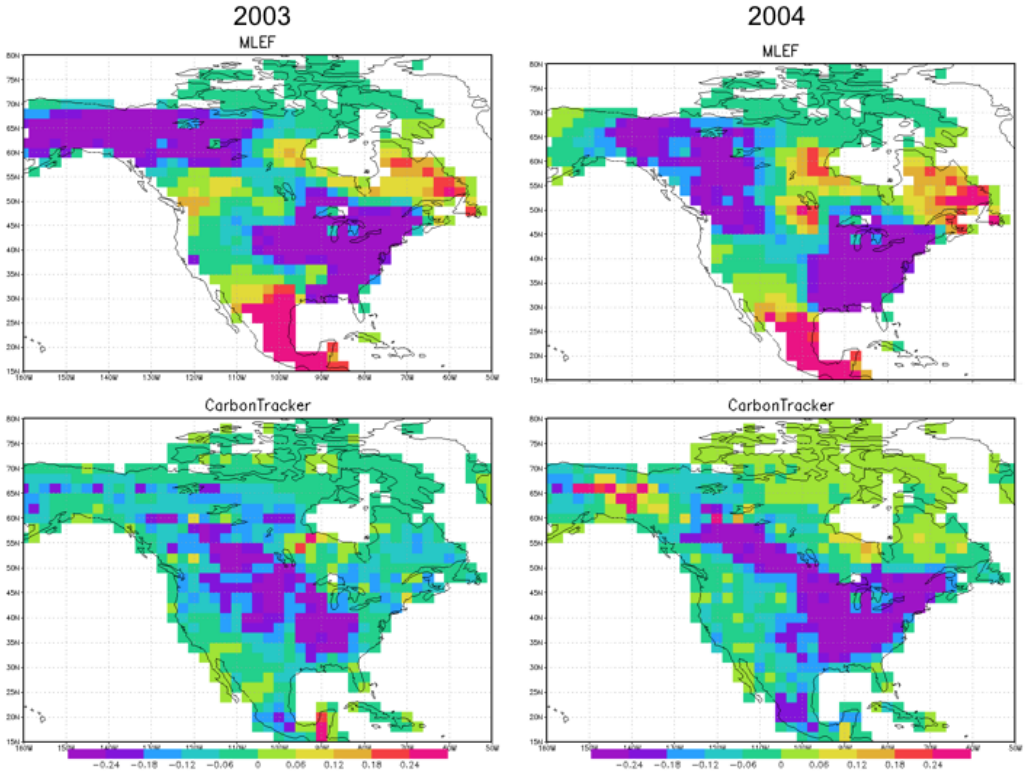

Figure 8. Mean annual NEE for North America estimated by MLEF and CarbonTracker for years 2003 and 2004. Units: moles/m^2/Sec.

We have tested the ensemble assimilation system using synthetic OCO data. Multiplicative biases (b) were specified to represent reasonable spatial patterns associated with CO2 fertilization, atmospheric nitrogen deposition, forest regrowth, boreal growing season changes, and a saturating sink in the Southern Ocean. Random grid-scale perturbations were added to each of these biases in each month, and synthetic CO2 data were created. Atmospheric columns were then sampled along the OCO orbit and masked for subgrid-scale clouds using NCEP-2 reanalyses. The resulting observation density is shown in Fig 9.

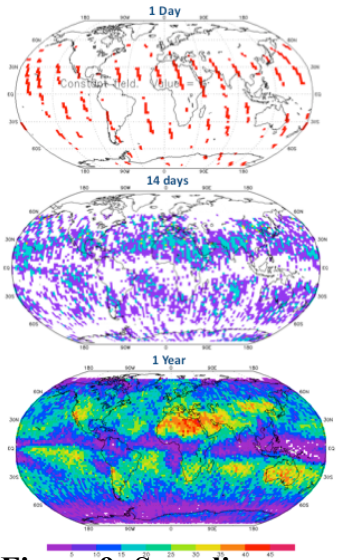

Figure 9: Sampling density for OSSE

A constant prior bias of $\beta(x,y,t)=0.0$ was assumed for all flux components, and new biases were estimated every month, with covariance propagation. Resulting fluxes were well-estimated (Fig 10) with excellent reduction of uncertainty over land. Ocean fluxes were somewhat less well-determined, due to the weaker fluxes there. (Fig 11)

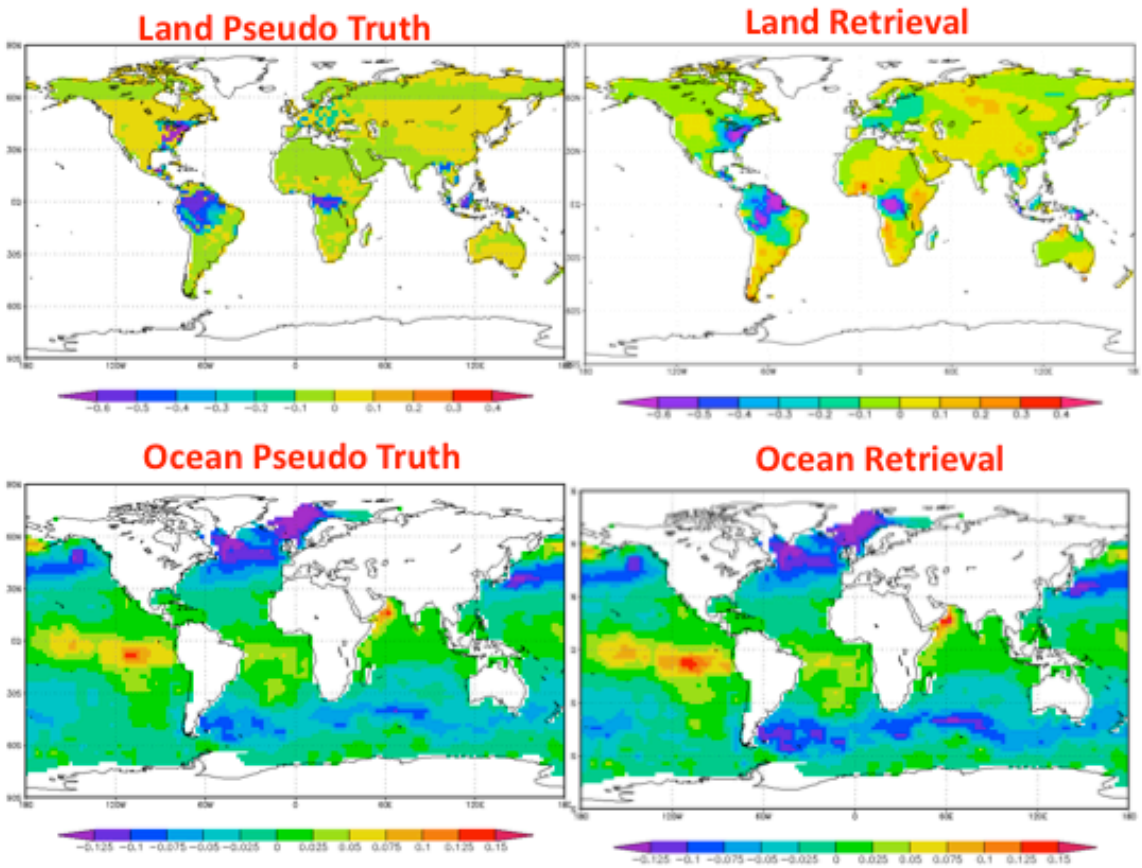

Figure 10: "True" and estimated fluxes (μMol CO_2 m^{-2} s^{-1}) recovered in OSSE

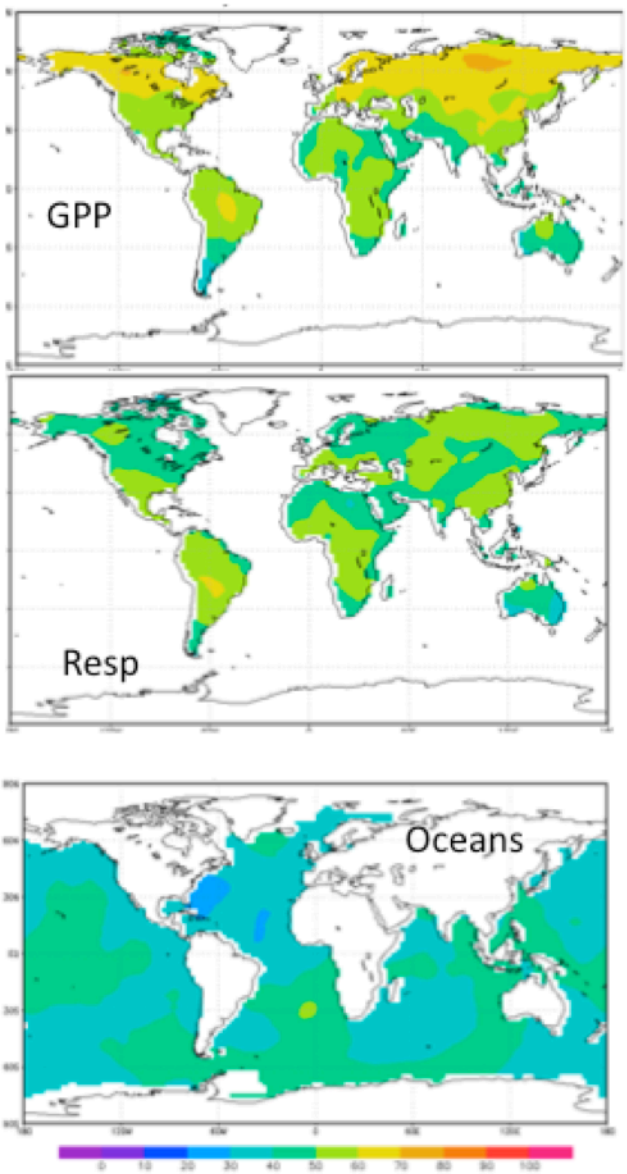

Figure 11: Uncertainty reduction (percent) relative to OSSE prior.

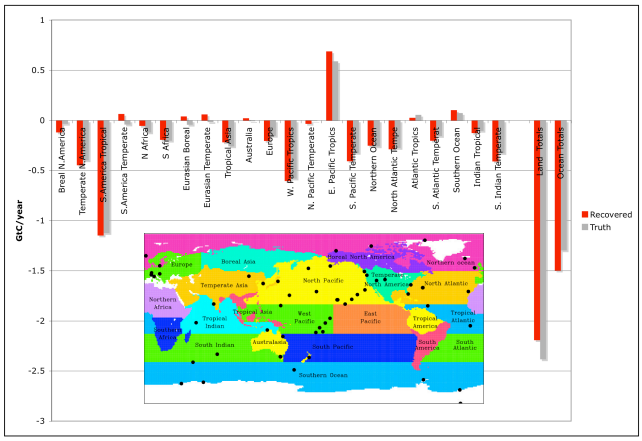

Figure 12: Post-aggregated flux estimates by TransCom region for OSSE compared to pseudo-truth (inset shows regions). Note that all land (but not ocean) priors were zero.

An important advantage of the MLEF system is that we are able to "post-aggregate" fluxes and their uncertainties a posteriori using the error covariance statistics that result from the optimization. Doing this shows excellent retrieval of annual fluxes over TransCom regions (Fig 12). Note that prior fluxes over all land regions were precisely zero due to the net annual balance architecture of SiB.

4. Publications and Presentations in Year 2

Baker, I.T., A.S. Denning, L. Prihodko, K. Schaefer, J.A. Berry, G.J. Collatz, N.S. Suits, R. Stockli, A. Philpott, O. Leonard, 2009: Global Net Ecosystem Exchange (NEE) of CO2, Available on-line [http://www.daac.ornl.gov] from Oak Ridge National Laboratory Distributed Active Archive Center, Oak Ridge, Tennessee, U.S.A.

Butler, M. P., K. J. Davis, A. S. Denning, and S. R. Kawa, 2010. Using continental observations in global atmospheric inversions of CO_2: 1. North American carbon sources and sinks. Submitted to *Tellus.*

A. S. Denning, R. Lokupitiya1, D. Zupanski1, N. Parazoo, D. Baker, S. Doney, I. Baker, R. Kawa, G. J. Collatz, S. Pawson, and K. Gurney, 2009. Carbon cycle data assimilation in the GOSAT era: An observing system simulation. Presented at the American Geophysical Union Fall 2009 Meeting, San Francisco CA, USA.

A. S Denning, N. Cavallaro, C. Ste-Marie, A. Muhlia-Melo. CarboNA: International studies of the North American carbon cycle. Invited Presentation at the American Geophysical Union Spring 2009 Meeting, Toronto, Canada.

J A Berry, J E Campbell, S A Montzka, S R Kawa, I Baker, A S Denning, A Wolf. Atmospheric measurements of co-variation carbonyl sulfide and carbon dioxide provide information on carbon cycle processes. Presentation at the American Geophysical Union Spring 2009 Meeting, Toronto, Canada.